

Supporting Information

Sekiya and Suzuki 10.1073/pnas.1016122108

SI Materials and Methods

Reagents. We injected 100 μ L of recombinant human HGF (100 μ g/mL; PeproTech) and 100 μ L of recombinant human IL-6 (100 μ g/mL; PeproTech) once at 1 d before analysis; 50 μ L of cholic acid (40 mg/mL; Nacalai Tesque) once a day for 4 d before analysis; 50 μ L of MG132 (10 mM; Peptide Institute) three times after PH; 50 μ L of SB415286 (10 mg/mL; Sigma-Aldrich) twice a day after PH; and 50 μ L of SB431542 (10 mg/mL; Sigma-Aldrich) once a day at 2 and 3 d after PH into the peritoneal cavity of 10-wk-old adult mice.

Western Blotting. Liver tissues were homogenized in lysis buffer comprising 50 mM Tris-HCl (pH 8.0), 150 mM NaCl, 1 mM EDTA, 0.5% Nonidet P-40, protease inhibitor mixture (Nacalai Tesque), and phosphatase inhibitor mixture (Calbiochem). To purify ubiquitin-binding proteins, the cell lysates were incubated with a ubiquitin-agarose affinity resin (Sigma-Aldrich) at 4 °C overnight. Cytoplasmic and nuclear protein fractions of adult hepatocytes that were isolated after two-step collagenase digestion (1) were obtained using an NE-PER Nuclear and Cytoplasmic Extraction Kit (Thermo-Pierce). For immunoprecipitation, the cell lysates were incubated with a goat anti-Snail antibody (Santa Cruz Biotechnology) at 4 °C overnight with gentle shaking, followed by incubation with protein G beads (GE Healthcare) for 2 h. The cell lysates were then subjected to SDS/PAGE, and the separated proteins were transferred to Immobilon-P membranes (Millipore). The membranes were incubated with primary antibodies at 4 °C overnight with gentle shaking. The following primary antibodies were used: goat anti-Snail, mouse anti-PCNA, mouse anti-cyclin D1, rabbit anti-cyclin D2, rabbit anti-cyclin D3, rabbit anti-cyclin A, rabbit anti-cyclin E, rabbit anti-CDK2, rabbit anti-CDK4, and goat anti-CYP7A1 (Santa Cruz Biotechnology); rabbit anti-GSK-3 β , rabbit antiphosphorylated GSK-3 β (Ser⁹), mouse anti-STAT-3, rabbit antiphosphorylated STAT-3 (Tyr⁷⁰⁵), and rabbit anti-histone H3 (Cell Signaling); mouse anti-E-cadherin, mouse anti-p21^{CIP1}, and mouse anti-p27^{KIP1} (BD Biosciences); mouse anti- β -actin (Abcam); goat anti-albumin (Bethyl Laboratories); mouse anti- α -smooth muscle actin (Sigma-Aldrich); and mouse antiphosphorylated serine (Calbiochem). The membranes were then washed with TBS containing 0.1% Tween-20 (Nacalai Tesque) and incubated with HRP-conjugated secondary antibodies specific to the appropriate species (1:2,000; Dako) for 2 h at room temperature. Finally, the immune complexes were visualized with ChemiLumi-One (Nacalai Tesque). The blots shown are representative of three experiments. The optical density of each band was measured using ImageJ software and normalized to that of the corresponding β -actin band.

Immunostaining. Frozen sections of liver tissues were initially fixed with 4% paraformaldehyde for 5 min and then fixed with methanol for 5 min at room temperature. After washing in PBS with 0.1% Tween-20 and blocking, the sections were incubated with the following primary antibodies: mouse anti-BrdU (Amersham), rabbit antigitlutamine synthetase (GS) (Abcam), guinea pig anti-CK8/18 (Progen), and rabbit anticlaved caspase-3 (Cell Signaling). Cultured cells were fixed using a Cytifix/Cytoperm Kit (BD Biosciences) and incubated with a mouse anti-BrdU antibody (BD Biosciences). To investigate E-cadherin expression, cells were

fixed as described previously (2) and incubated with a mouse anti-E-cadherin antibody (BD Biosciences). After washing, the sections and cells were incubated with Alexa 488- and/or Alexa 555-conjugated secondary antibodies specific to the appropriate species (1:200; Molecular Probes), followed by nuclear staining with DAPI.

Expression Constructs and siRNA. The entire coding sequence of mouse GSK-3 β was obtained by RT-PCR using 13.5-dpc mouse embryonic liver-derived total RNA and then inserted into pIRES2-GFP (Clontech). Total RNA was prepared using an RNeasy Mini Kit (Qiagen) according to the manufacturer's instructions. KD-GSK-3 β /pIRES2-GFP was generated from GSK-3 β /pIRES2-GFP by PCR (primers: 5'-aactggttccatcatgatgttctacaggacaa-3' and 5'-ttgtcctgtagaactatcatgatggcaaccagt-3'). Snail siRNA, Snail-control siRNA, GSK-3 β siRNA, and GSK-3 β -control siRNA (Stealth RNAi, target sequences: 5'-cagtcgccaaga-tcttcaactga-3', 5'-cagggcgagaattctcaacttca-3', 5'-gacacacctgca-cttcaactta-3', and 5'-gactcacaacttctcaactcatta-3', respectively) were designed and synthesized (Invitrogen).

Hydrodynamic Gene Delivery and Cell Transfection. Naked plasmid DNA (50 μ g) or siRNA (50 μ g) was intravascularly injected from the spleen into mice using TransIT-EE (Mirus Bio) or TransIT-QR (Mirus Bio), respectively, according to the manufacturer's instructions. Transfection of hepatic progenitor cell cultures was carried out with Lipofectamine 2000 (Invitrogen).

Gene Expression Analysis. qPCR was conducted as described previously (3). We used qPCR primers and probes for *Snail* (TaqMan Gene Expression Assay ID: Mm00441533_g1; Applied Biosystems), *GSK-3 β* (TaqMan Gene Expression Assay ID: Mm00444911_m1; Applied Biosystems), and *E-cadherin* (TaqMan Gene Expression Assay ID: Mm00486909_g1; Applied Biosystems).

Flow Cytometry and Cell Culture. Hepatic progenitor cells were prospectively isolated from the liver of 13.5-dpc mouse embryos and clonally cultured as described previously (4). BrdU-incorporating cells were stained using an APC BrdU Flow Kit (BD Biosciences). The fluorescently labeled cells were analyzed and separated with a FACS Aria (BD Biosciences).

Chromatin Immunoprecipitation Assay. Cells obtained from homogenized liver tissues were fixed with 1% paraformaldehyde for 10 min at room temperature. Cell lysates were prepared, sonicated, and immunoprecipitated with a goat anti-Snail antibody (Santa Cruz Biotechnology). A 200-bp DNA fragment containing an E-box consensus for Snail binding in the *cyclin D2* promoter, which is conserved between mouse and human (5), was amplified by PCR with primers 5'-ctagcctaagcgtccctgatca-3' and 5'-cgttt-cctcactctctctgct-3'.

Measurement of Alanine Transaminase. Alanine transaminase in mouse plasma was detected using an Alanine Transaminase Activity Assay Kit (Cayman Chemical) according to the manufacturer's instructions. The absorbance signals were measured with a Multiskan FC microplate reader (Thermo Fisher Scientific).

1. Seglen PO (1979) Hepatocyte suspensions and cultures as tools in experimental carcinogenesis. *J Toxicol Environ Health* 5:551-560.

2. Suzuki A, Nakauchi H, Taniguchi H (2003) Glucagon-like peptide 1 (1-37) converts intestinal epithelial cells into insulin-producing cells. *Proc Natl Acad Sci USA* 100:5034-5039.

3. Suzuki A, Iwama A, Miyashita H, Nakauchi H, Taniguchi H (2003) Role for growth factors and extracellular matrix in controlling differentiation of prospectively isolated hepatic stem cells. *Development* 130:2513–2524.

4. Suzuki A, et al. (2002) Clonal identification and characterization of self-renewing pluripotent stem cells in the developing liver. *J Cell Biol* 156:173–184.

5. Vega S, et al. (2004) Snail blocks the cell cycle and confers resistance to cell death. *Genes Dev* 18:1131–1143.

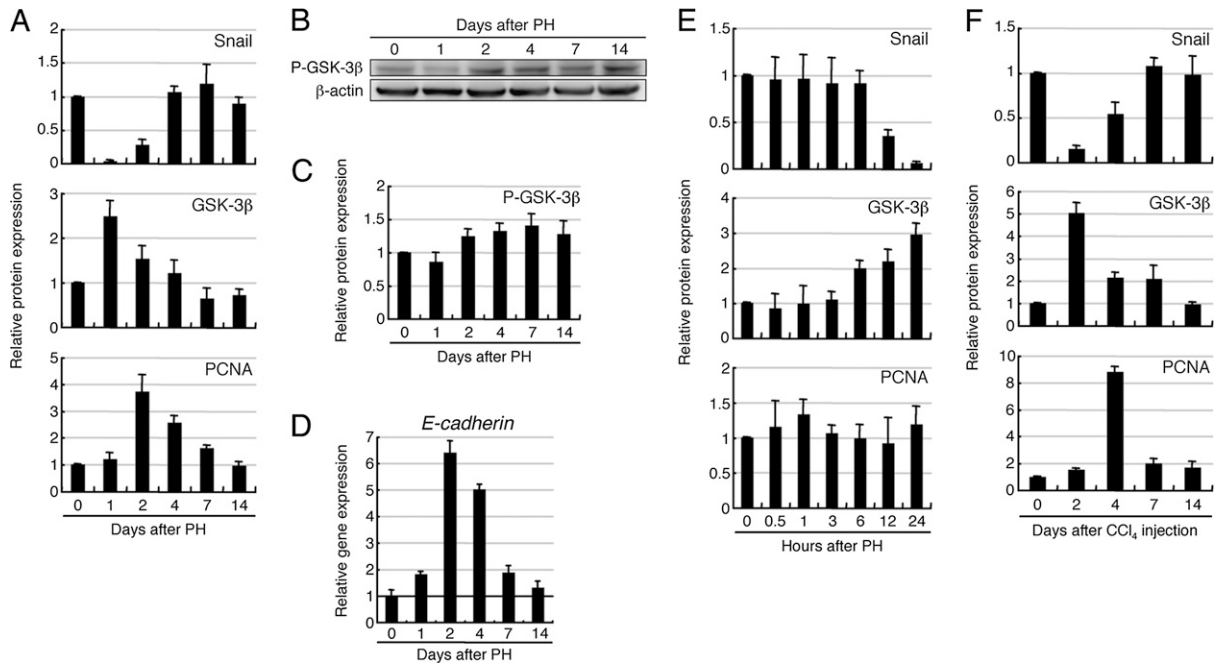


Fig. S1. (A) Quantification of Western blots for Snail, GSK-3β, and PCNA in the liver after PH. (B) Western blot analyses of serine 9-phosphorylated GSK-3β (P-GSK-3β) in the liver after PH. (C) Quantification of Western blots for P-GSK-3β in the liver after PH. (D) qPCR analyses of *E-cadherin* were carried out on total RNA derived from the liver after PH. (E) Quantification of Western blots for Snail, GSK-3β, and PCNA in the liver after PH. (F) Quantification of Western blots for Snail, GSK-3β, and PCNA in the liver after CCl₄ injection. The data shown in A, C, and D–F were normalized by the value of the liver at 0 d/h after PH or CCl₄ injection, respectively, and the fold differences are shown. The data are means ± SD (*n* = 3).

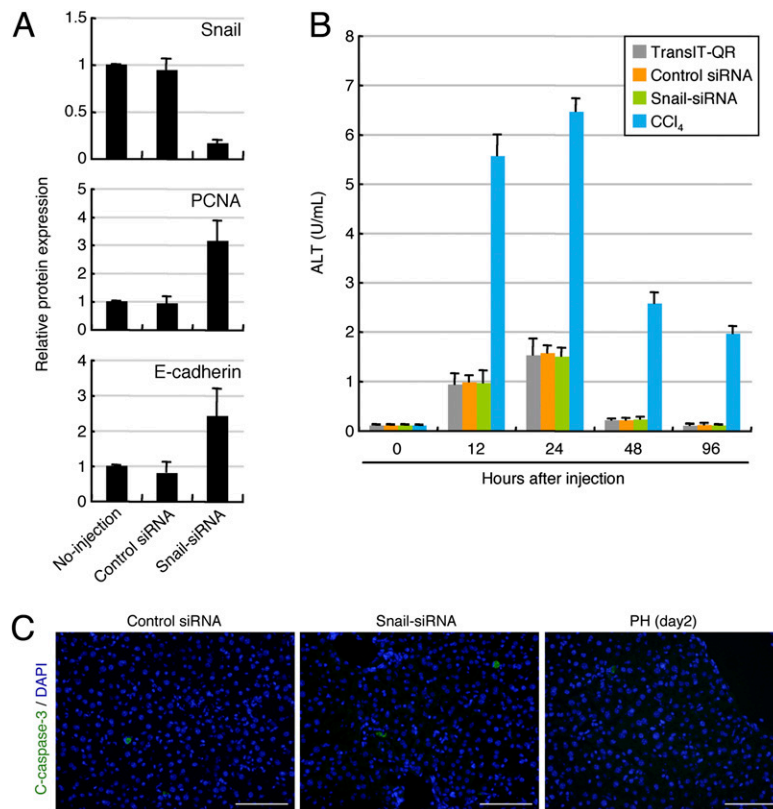


Fig. S2. (A) Quantification of Western blots for Snail, PCNA, and E-cadherin in age-matched normal mouse liver (no injection) and in the liver of adult mice at 2 d after hydrodynamic injection of a control siRNA or Snail siRNA. All data were normalized by the value of age-matched normal mouse liver (no injection), and the fold differences are shown. The data are means \pm SD ($n = 3$). (B) The level of alanine transaminase (ALT) in mouse plasma after injection of TransIT-QR, a control siRNA, Snail siRNA, or CCl₄. Hydrodynamic injection of TransIT-QR, a control siRNA, or Snail siRNA temporally induced an increase in the level of ALT, but its level was much lower than the level of ALT after CCl₄ injection. The data are means \pm SD ($n = 3$). (C) Immunofluorescence staining of cleaved caspase-3 revealed that there was little increase in the number of apoptotic cells in the liver at 2 d after injection of a control siRNA or Snail siRNA and at 2 d after PH. DNA was stained with DAPI. (Scale bars, 100 μ m.)

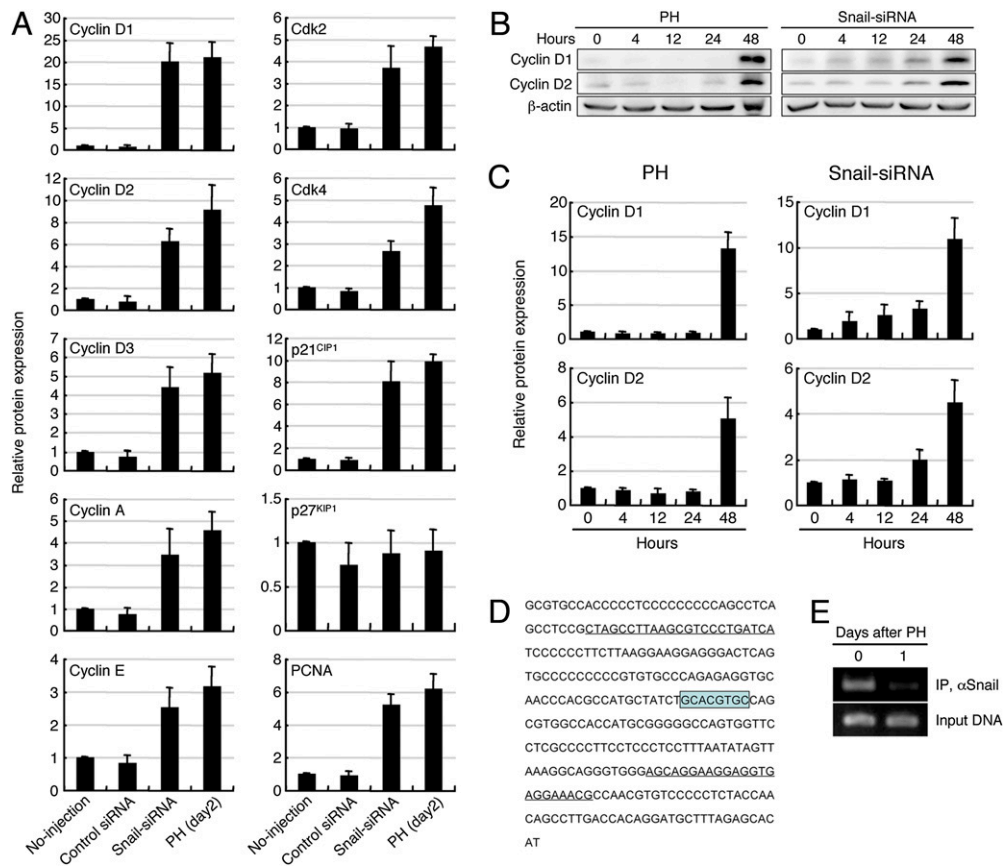


Fig. 53. (A) Quantification of Western blots for cell cycle-related proteins in age-matched normal mouse liver (no injection) and in the liver of adult mice at 2 d after hydrodynamic injection of a control siRNA or Snail siRNA and at 2 d after PH. All data were normalized by the value of age-matched normal mouse liver (no injection), and the fold differences are shown. The data are means \pm SD ($n = 3$). (B and C) Time-course changes in the amounts of cyclin D1 and cyclin D2 in the liver after PH or Snail siRNA injection. (B) Western blot analyses of cyclin D1 and cyclin D2 in the liver after PH or Snail siRNA injection. (C) Quantification of Western blots for cyclin D1 and cyclin D2 in the liver after PH or Snail siRNA injection. All data were normalized by the value of the liver at 0 h after PH or Snail siRNA injection, and the fold differences are shown. The data are means \pm SD ($n = 3$). (D) Sequence between base pairs $-1,623$ and $-1,324$ upstream of the translation start of the mouse *cyclin D2* gene. The core sequence 5'-GCACGTGC-3' contained in an E-box of the mouse *cyclin D2* promoter is indicated by box. Underlines show the sequence of primers. (E) ChIP assays were carried out on cell lysates derived from the liver of adult mice at 0 and 1 d after PH. (Lower) PCR amplification of input DNA before immunoprecipitation. Representative data in three experiments are shown.

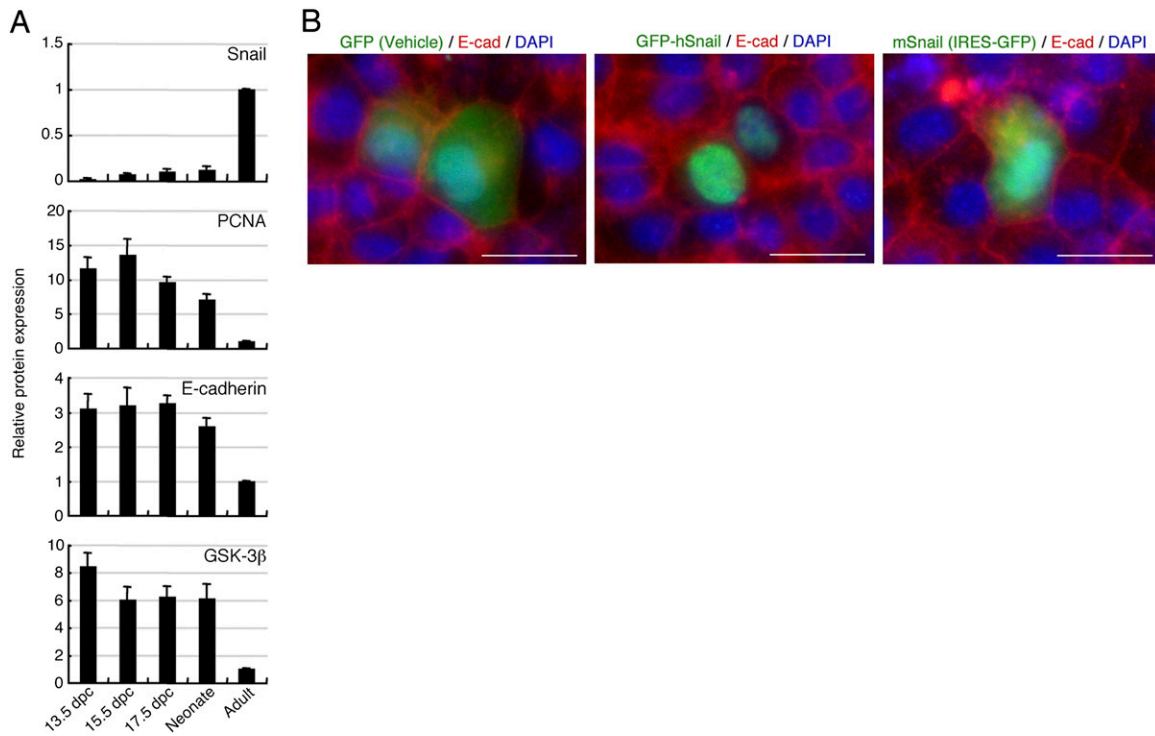


Fig. 54. (A) Quantification of Western blots for Snail, PCNA, E-cadherin, and GSK-3 β in the liver of embryonic (13.5, 15.5, and 17.5 dpc), neonatal (postnatal day 1), and 10-wk-old adult mice. All data were normalized by the value of the adult mouse liver, and the fold differences are shown. The data are means \pm SD ($n = 3$). (B) Immunofluorescence staining of E-cadherin revealed that, even after transfection of a construct that expressed mouse or human *Snail* with GFP, E-cadherin was expressed and typically localized at sites of cell–cell junctions in hepatic progenitor cells. Vehicle-transfected cells were evaluated as a control. DNA was stained with DAPI. (Scale bars, 25 μ m.)

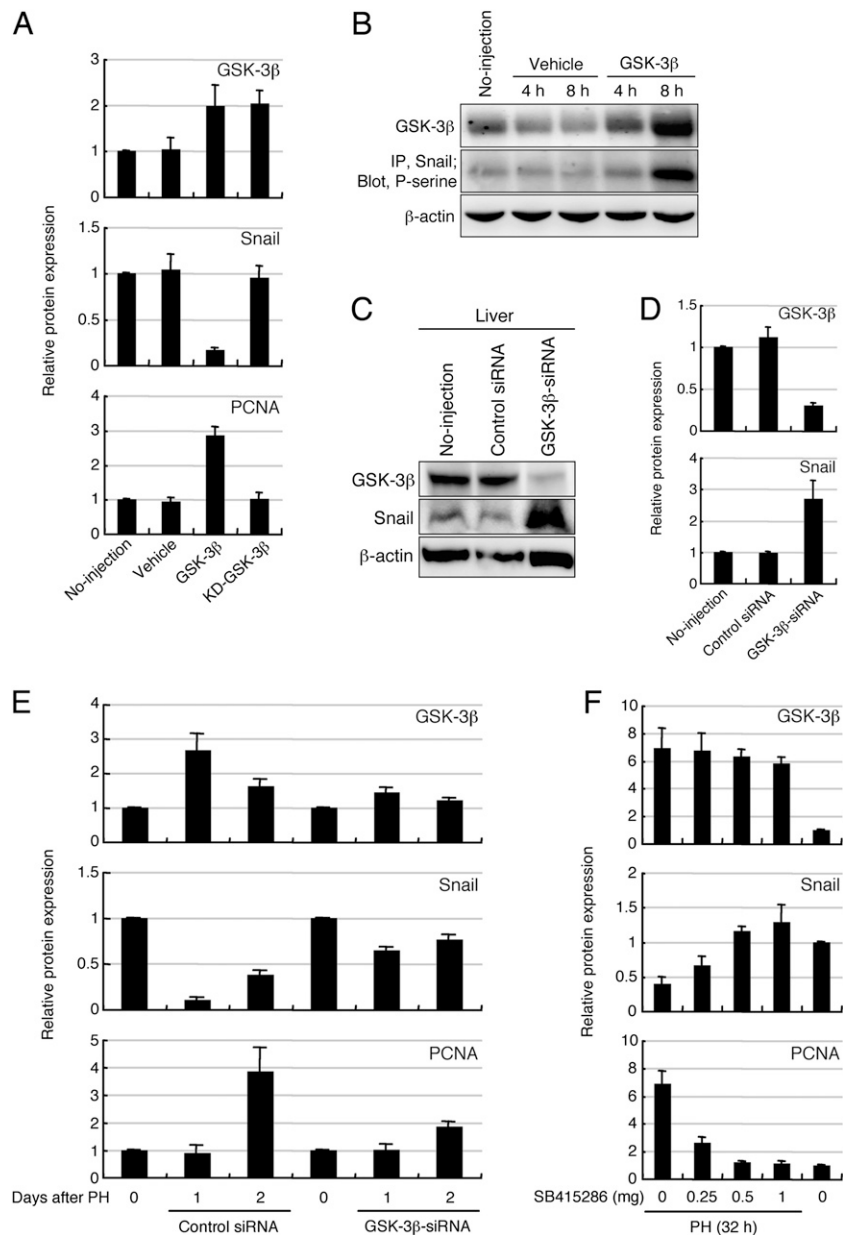


Fig. 55. (A) Quantification of Western blots for GSK-3β, Snail, and PCNA in age-matched normal mouse liver (no injection) and in the liver of adult mice at 1 d after hydrodynamic injection of vehicle, wild-type GSK-3β expression construct, or KD-GSK-3β expression construct. (B) An increased amount of GSK-3β in the liver promotes the phosphorylation of serine residues within Snail. Cell lysates were prepared from age-matched normal mouse liver (no injection) and from the liver of adult mice at 4 and 8 h after hydrodynamic injection of vehicle or a GSK-3β expression construct. Immunoprecipitations of the cell lysates were performed with an anti-Snail antibody, followed by Western blotting with an antiphosphorylated serine (P-serine) antibody. Western blot analysis of GSK-3β was also carried out on these cell lysates. IP, immunoprecipitation; P, phosphorylated. (C) Western blot analyses of GSK-3β and Snail in age-matched normal mouse liver (no injection) and in the liver of adult mice at 2 d after hydrodynamic injection of a control siRNA or GSK-3β siRNA. (D) Quantification of Western blots for GSK-3β and Snail in age-matched normal mouse liver (no injection) and in the liver of adult mice at 2 d after hydrodynamic injection of a control siRNA or GSK-3β siRNA. (E) Quantification of Western blots for GSK-3β, Snail, and PCNA in the liver after PH, following the introduction of a control siRNA or GSK-3β siRNA into adult mice by hydrodynamic injection at 1 d before PH. (F) Quantification of Western blots for GSK-3β, Snail, and PCNA in the liver of SB415286-treated mice at 32 h after PH and in age-matched normal mouse liver. The data shown in A and D–F were normalized by the value of age-matched normal mouse liver (no injection) or the liver at 0 d after PH, respectively, and the fold differences are shown. The data are means ± SD (n = 3).

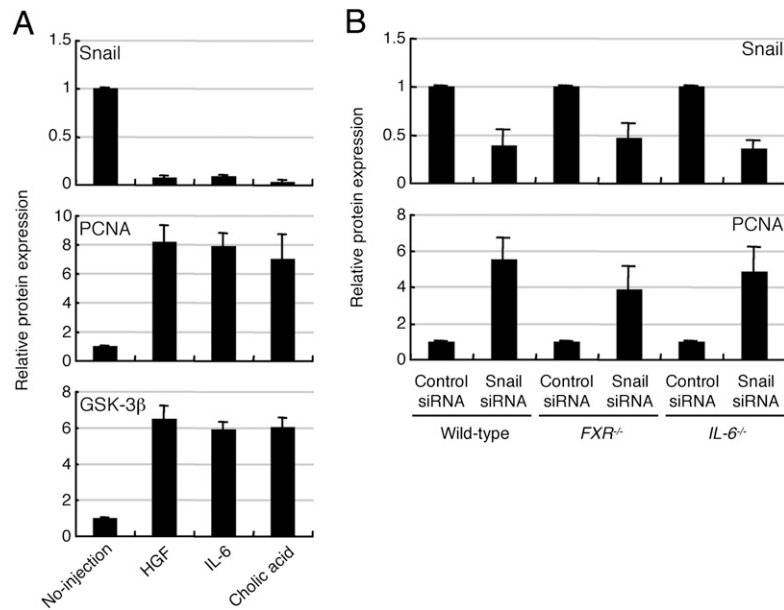


Fig. 56. (A) Quantification of Western blots for Snail, PCNA, and GSK-3β in age-matched normal mouse liver (no injection) and in the liver of adult mice at 1 d after injection of HGF, IL-6, and cholic acid. (B) Quantification of Western blots for Snail and PCNA in the liver of wild-type, *FXR*^{-/-}, and *IL-6*^{-/-} mice at 2 d after hydrodynamic injection of a control siRNA or Snail siRNA into adult mice. The data shown in A or B was normalized by the value of age-matched normal mouse liver (no injection) or the liver of control siRNA-injected mice, respectively, and the fold differences are shown. The data are means ± SD ($n = 3$).

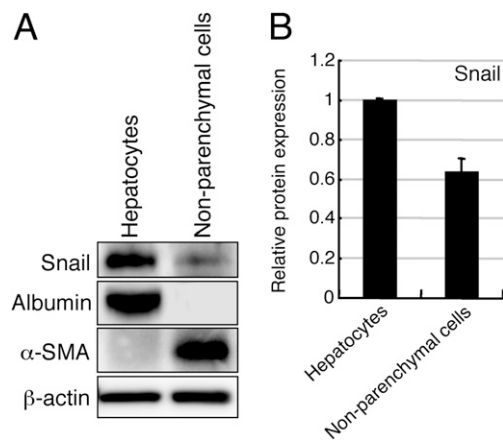


Fig. 57. Snail is expressed in both hepatocytes and nonparenchymal cells in the adult mouse liver, but its expression level in hepatocytes is higher than that in nonparenchymal cells. (A) Western blot analyses of Snail, albumin, and α-smooth muscle actin (SMA) in hepatocytes and nonparenchymal cells. Albumin and α-SMA, which are expressed in hepatocytes and nonparenchymal cells, respectively, were evaluated to confirm the separation of hepatocytes and nonparenchymal cells. (B) Quantification of Western blots for Snail in hepatocytes and nonparenchymal cells. All data were normalized by the value of hepatocytes, and the fold differences are shown. The data are means ± SD ($n = 3$).

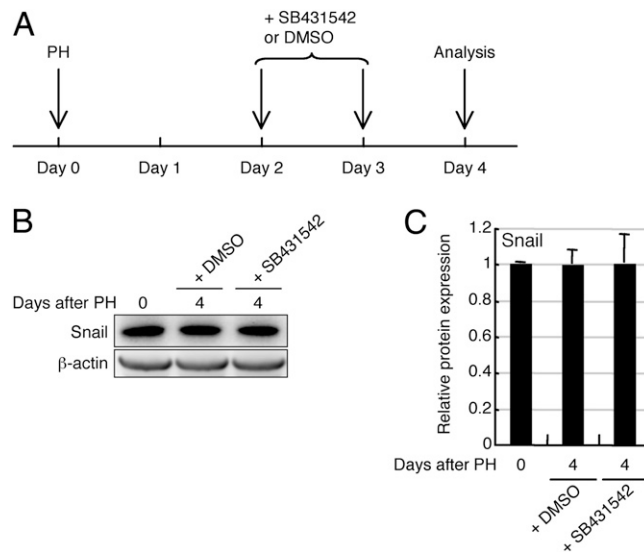


Fig. S8. Inhibition of TGF β signaling cannot suppress up-regulation of Snail following its transient degradation after PH. **(A)** Experimental procedures to elucidate the role of TGF β signaling in Snail expression in the liver after PH. **(B)** Western blot analyses of Snail in the liver of adult mice at 0 d after PH and in the liver of DMSO or SB431542-treated mice at 4 d after PH. **(C)** Quantification of Western blots for Snail in the liver of adult mice at 0 d after PH and in the liver of DMSO or SB431542-treated mice at 4 d after PH. All data were normalized by the value of the liver at 0 d after PH, and the fold differences are shown. The data are means \pm SD ($n = 3$).

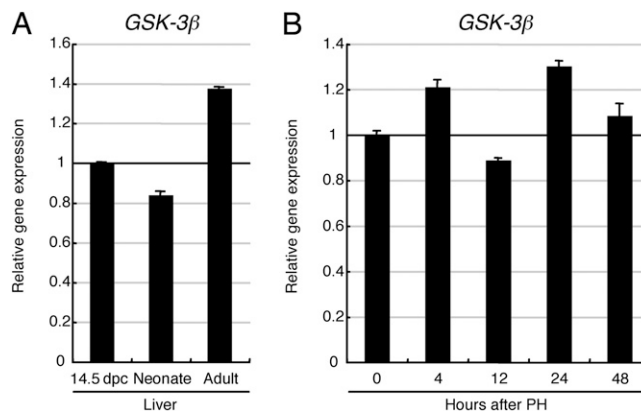


Fig. S9. There is little change in the level of GSK-3 β mRNA expression during liver development and regeneration. **(A and B)** qPCR analyses of *GSK-3 β* were carried out on total RNA derived from 14.5-dpc, neonatal (postnatal day 1), and 10-wk-old adult mouse livers **(A)** and from the liver after PH **(B)**. The data shown in **A** and **B** were normalized by the values of the 14.5-dpc mouse liver or the liver at 0 h after PH, respectively, and the fold differences are shown. The data are means \pm SD ($n = 3$).